



# MIT Open Access Articles

## *Comparison of scintillation measurements from a 5 km communication link to standard statistical models*

The MIT Faculty has made this article openly available. **Please share** how this access benefits you. Your story matters.

<b>Citation</b>	Michael, Steven et al. "Comparison of scintillation measurements from a 5 km communication link to standard statistical models." Atmospheric Propagation VI. Ed. Linda M. Wasiczko Thomas & G. Charmaine Gilbreath. Orlando, FL, USA: SPIE, 2009. 73240J-7. © 2009 SPIE
<b>As Published</b>	<a href="http://dx.doi.org/10.1117/12.819006">http://dx.doi.org/10.1117/12.819006</a>
<b>Publisher</b>	Society of Photo-Optical Instrumentation Engineers
<b>Version</b>	Final published version
<b>Citable link</b>	<a href="http://hdl.handle.net/1721.1/52635">http://hdl.handle.net/1721.1/52635</a>
<b>Terms of Use</b>	Article is made available in accordance with the publisher's policy and may be subject to US copyright law. Please refer to the publisher's site for terms of use.

# Comparison of Scintillation Measurements from a 5 km Communication Link to Standard Statistical Models

Steven Michael, Ronald R. Parenti, Frederick G. Walther, Alicia M. Volpicelli, John D. Moores, William Wilcox Jr., and Robert Murphy

MIT Lincoln Laboratory, 244 Wood St., Lexington, MA 02420, USA.

## ABSTRACT

As part of a free-space optical communications experiment over a 5km horizontal path, an extensive database of tilt-stabilized receiver data was collected for  $C_n^2$  conditions ranging from benign to very strong. This paper focuses on the scintillation measurements made during those tests. Ensemble probability distributions are compiled from these results, and are subsequently compared with standard channel models such as the log-normal and gamma-gamma distributions. Statistical representations of temporal behavior are also developed from this database. Accurate statistical models of atmospheric channel effects have proved to be invaluable in the development of high-performance free-space transceivers.

**Keywords:** Atmospheric Turbulence, Diversity, Lasercom, Gamma-Gamma Distribution

## 1. INTRODUCTION

The use of optical carrier wavelengths for wireless communications offers the potential of high bandwidth links with size, weight, and power (SWaP) significantly smaller than radio frequency links of comparable bandwidth. Assuming line-of-site requirements can be met, stochastic thermally induced refractive index fluctuations in the free atmosphere present the most difficult challenge to implementing such links. These fluctuations produce optical path differences over the signal cross-section that can be a significant fraction of an optical wavelength. The resulting phase aberrations diffract to become intensity fluctuations, known as scintillation, in the far field. A point receiver in the far field will see time varying irradiance that can vary by tens of decibels above and below the mean.

A robust optical terminal design must ensure error-free communications over the wide dynamic range of received powers. Increasing the transmitter aperture size and optical power deliver higher irradiance at the expense of terminal SWaP. The use of large or multiple receive apertures that sample independent uncorrelated intensity patches reduces the dynamic range of total received power, keeping it above the receiver sensitivity most or all of the time. Should received power drop below receiver sensitivity, forward error correction (FEC) and interleaving can combine to correct the resulting errors. Choosing an operating point within this large parameter space requires understanding the statistics of atmosphere-induced power variation.

Andrews, Phillips, Hopen, and Al-Habash<sup>1</sup> have developed a heuristic model based upon a modification of the Rytov method to describe scintillation statistics (hereafter referred to as the Andrews model). They propose using the gamma-gamma distribution to describe probabilities of received irradiance. The two free parameters of this distribution are derived from the refractive index structure parameter,  $C_n^2$ , along the optical path, and possibly the size of the inner scale size,  $l_0$ , and outer scale,  $L_0$ . The gamma-gamma distribution has been tested against wave-optics simulations,<sup>1,2</sup> and to a lesser extent experimental data.<sup>3,4</sup> It is becoming widely used as basis for predicting link performance for a variety of terminals, coding techniques, and link geometries.<sup>5-7</sup>

In this paper, we test the gamma-gamma model predictions against measured distributions from a deployed optical link. In the summer and fall of 2008, MIT Lincoln Laboratory deployed an experimental link seeking to demonstrate robust performance against a wide range of atmospheric conditions. The link included a point source transmitter and point receiver separated by a well characterized path. Transmit and received powers were sampled at high rate over the course of the 1.5 month deployment. Over 120 hours of total data have

---

Send correspondence to: Steven Michael, smichael@ll.mit.edu

been collected, completely covering the large diurnal variation of turbulence strength. This permits testing the spherical wave predictions of the model against experimental data for  $C_n^2$  values varying by over two orders of magnitude.

The next section provides a more detailed description of our experiment. We follow with a brief description of how scintillation drives network availability. In section 4 we give a more detailed description of the gamma-gamma model, and in section 5 we present and discuss comparisons of our data to the model predictions.

## 2. OVERVIEW OF EXPERIMENT

MIT Lincoln Laboratory deployed an OTU-1 (2.667 Gbaud) 1550 nm free-space optical link between two ground sites spanning a 5.4 km distance. A single 12 mm diameter transmitter located on a fire tower in Groton, MA provided signal to 4 identical 12 mm diameter receivers located within the Firepond observatory in Westford, MA. Each receiver independently tracked the incoming beam and coupled the received power into a single mode fiber. Narrow beams of differing wavelengths were returned from each receiver along the measured line of site back to the transmitter, allowing for cooperative tracking. The photocurrents from each receiver were combined to provide a summed signal to a RZ-OOK transceiver. Custom hardware provided error correction and interleaving with variable interleaver spans that were programmable to values exceeding 1 second. Maximum transmit power was 16.7 dBm. The spatial averaging of scintillation from multiple receivers and temporal averaging from the interleaver provided robust link performance for all observed fading conditions.

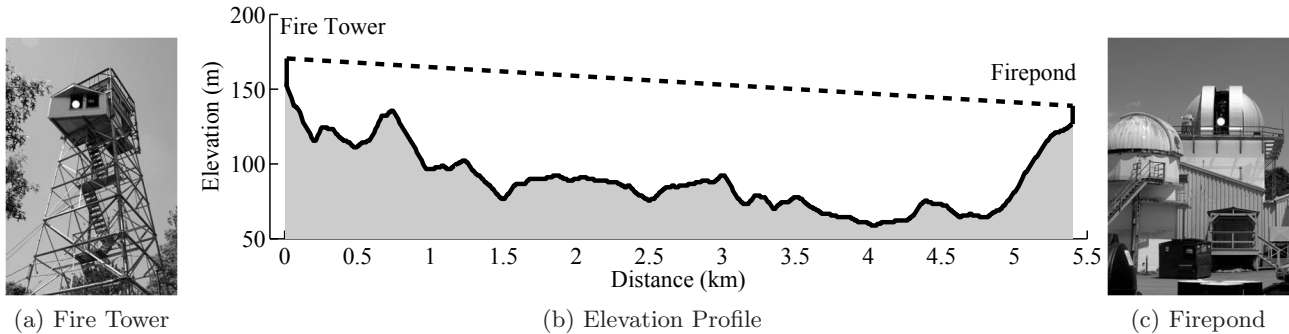


Figure 1: Transmitter, receiver, and path profile

As Figure 1 shows, the transmitter and receivers are located about 20 m off the ground and on average the path is 75 m above ground level. The terrain along the path is mostly foliage; we expect  $C_n^2$  to be relatively constant along the line of site. Additional instrumentation allows for a detailed characterization and recording of the dynamic atmospheric conditions during link operation. A Scintec BLS900 scintillometer<sup>8</sup> aligned co-linear with the link path provides an independent characterization of the atmospheric channel. Temperature, wind speed, and wind direction are monitored at 5 second intervals by weather stations located at each end of the path. Transmit power and power in fiber for each receiver are sampled and recorded at 1 millisecond intervals by New Focus 2103 power meters having 75 dB of dynamic range. A focal plane array within each receiver measures track error signal and provides a measure of power in aperture with 20 dB dynamic range.

Even under the most turbulent atmospheric conditions, the 12 mm diameter of the receive apertures is much smaller than the coherence diameter of the atmosphere as measured by the commercial scintillometer and the scintillated intensity patch sizes as measured by a separate camera imaging the receiver plane. The wide transmitter divergence ( $160 \mu\text{rad}$ ) and small receiver diameter produce tilts at the receiver that are relatively small and easily corrected by the tracking system. As such, the power in aperture is always efficiently coupled into the single mode fiber. This combination of factors allows the sampled power in fiber to provide a high-rate, wide dynamic range measure of spherical wave atmospheric scintillation.

Figure 2 shows  $C_n^2$  for a typical sunny day, as measured along the link path by the Scintec scintillometer. Quiescent periods occur mid-morning and early-evening. The evening quiescent period is usually more benign than the morning. Over the course of a sunny day,  $C_n^2$  changes by more than two orders of magnitude, allowing us to sample a broad range of atmospheric conditions.

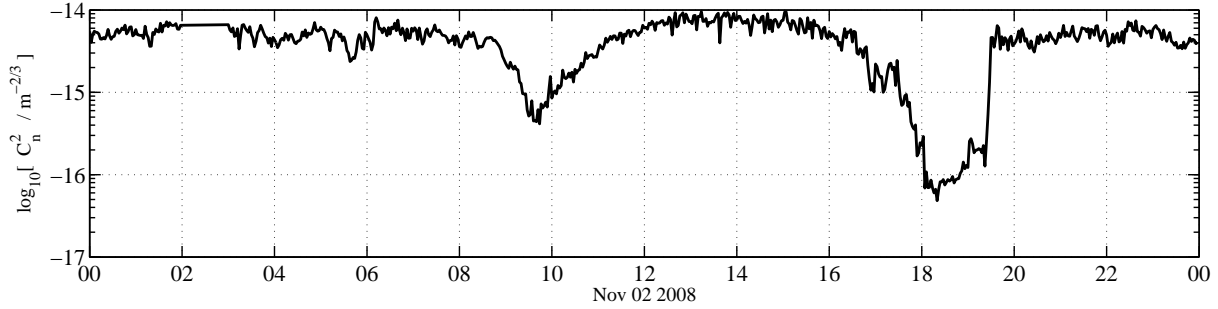


Figure 2:  $C_n^2$  for a typical sunny day.

### 3. NETWORK AVAILABILITY

A link outage occurs when the receiver is unable to recover faithfully the transmitted signal. With an FEC encoded signal, the uncorrectable bit error rate increases rapidly from zero over a very narrow range of received signal power. This power level is the receiver sensitivity  $P_s$ ; signal powers below this threshold will produce an outage. An acceptable outage rate will be determined by the availability requirements of a particular link; one outage per day or per hour might be typical.

The outage frequency  $f_o$  can be roughly estimated by the following equation:

$$f_o = \frac{P(P_R < P_s)}{\tau_c} \quad (1)$$

where  $\tau_c$  is the coherence time of the atmosphere and  $P(P_R < P_s)$  is the probability of signal power being less than the sensitivity of the receiver. A typical coherence time for our link is about 4 milliseconds. Coherence times for moving terminals such as one mounted on an airborne platform will be significantly shorter. For reasonable outage rates, this means the probability distribution must be known to the  $10^{-5}$  level or beyond. Modest FEC combined with an interleaver that spreads codeword symbols over many coherence times may bring this up to the  $10^{-3}$  level. The difference between the fade power at this probability and the mean power is the excess margin required by the link to ensure operation through scintillation-induced fading. This is the scintillation penalty.

The scintillation penalty is determined by the low-probability tails of the distribution. This can be mitigated by the use of FEC and interleaving, but low probability events will still drive outages. **A scintillation model must be accurate at these low probabilities to accurately predict network availability.**

### 4. ANDREWS MODEL

Andrews, Phillips, Hopen, and Al-Al-Habash have developed a heuristic model to describe the statistics of atmospheric scintillation. They propose a modified Kolmogorov spectrum that separates refractive index fluctuations into large and small scale terms that act independently on the field. Using modified Rytov theory, they develop expressions for  $\sigma_{\ln x}^2$  and  $\sigma_{\ln y}^2$ , the variances in the log-amplitude of the field arising from the large and small scale fluctuations, respectively. For a spherical wave in the absence of inner scale, these are given by:

$$\sigma_{\ln x}^2 \cong \frac{0.49\beta_0^2}{(1 + 0.56\beta_0^{12/5})^{7/6}}, \quad \sigma_{\ln y}^2 \cong \frac{0.51\beta_0^2}{(1 + 0.62\beta_0^{12/5})^{5/6}} \quad (2)$$

where  $\beta_0^2$  is the predicted irradiance variance relative to the mean for a spherical wave. For a constant  $C_n^2$  profile:

$$\beta_0^2 = 0.496C_n^2 k^{7/6} L^{11/6} \quad (3)$$

We note that for our link (see Figure 2),  $C_n^2$  ranges from  $1 \times 10^{-16} m^{-2/3}$  to  $2 \times 10^{-14} m^{-2/3}$ , producing  $\beta_0$  values that extend from benign turbulence,  $\beta_0 \cong 0.05$ , to saturation,  $\beta_0 \cong 1$ .

The expressions in equation (2) are derived using the Kolmogorov spectrum to describe index fluctuations. Hill<sup>9</sup> has described a more accurate spectrum in which power increases near  $2\pi/l_0$  before truncating at larger wavenumbers. Using a modified version of this spectrum leads to the following modified expression for large and small scale log-amplitude variances of a spherical wave:

$$Q_l = \frac{10.89L}{kl_0^2} \quad (4)$$

$$\begin{aligned} \sigma_s^2 = & 9.65\beta_0^2 \left\{ 0.40 (1 + 9/Q_l^2)^{11/12} \left[ \sin \left( \frac{11}{6} \tan^{-1} \left( \frac{Q_l}{3} \right) \right) \right. \right. \\ & + \frac{2.61}{(9 + Q_l^2)^{1/4}} \sin \left( \frac{4}{3} \tan^{-1} \left( \frac{Q_l}{3} \right) \right) \\ & \left. \left. - \frac{0.52}{(9 + Q_l^2)^{7/24}} \sin \left( \frac{5}{4} \tan^{-1} \left( \frac{Q_l}{3} \right) \right) \right] - \frac{3.50}{Q_l^{5/6}} \right\}, \beta_0^2 < 1 \end{aligned} \quad (5)$$

$$\begin{aligned} \sigma_{\ln x}^2 = & 0.04\beta_0^2 \left[ \frac{8.56Q_l}{8.56 + Q_l + 0.20\beta_0^2 Q_l^{7/6}} \right]^{7/6} \times \\ & \left[ 1 + 1.75 \left( \frac{8.56Q_l}{8.56 + Q_l + 0.20\beta_0^2 Q_l^{7/6}} \right)^{1/2} - 0.25 \left( \frac{8.56Q_l}{8.56 + Q_l + 0.20\beta_0^2 Q_l^{7/6}} \right)^{7/12} \right] \end{aligned} \quad (6)$$

$$\sigma_{\ln y}^2 = \frac{0.51\sigma_s^2}{\left(1 + 0.69\sigma_s^{6/5}\right)^{5/6}} \quad (7)$$

If the large and small scale irradiances are each described by a gamma distribution, the combined probability distribution is gamma-gamma:

$$p(I) = \frac{2(\alpha\beta)^{(\alpha+\beta)/2}}{\Gamma(\alpha)\Gamma(\beta)} I^{(\alpha+\beta)/2-1} K_{\alpha-\beta} \left( 2\sqrt{\alpha\beta}I \right) \quad (8)$$

This is parametrized by  $\alpha$  and  $\beta$ , representing the large and small scale fluctuations. By examining the second moment of the distribution, we find:

$$\alpha = \frac{1}{\exp(\sigma_{\ln x}^2) - 1} \quad , \quad \beta = \frac{1}{\exp(\sigma_{\ln y}^2) - 1} \quad (9)$$

The expressions above can be used to estimate the probability distribution of atmospheric scintillation knowing only the  $C_n^2$  profile and inner scale value for a given link geometry.

## 5. GAMMA-GAMMA FITS TO MEASURED SCINTILLATION

In this section we compare measured distributions of irradiance to those predicted by the Andrews heuristic model. We have chosen 9 data sets which span the space of observed atmospheric conditions. Each data set is 2 minutes in length, allowing us to generate distributions down to roughly  $10^{-5}$  probability. These data sets represent times where the  $C_n^2$  values as measured by the scintillometer are relatively static and the link is operating with full telemetry being recorded. An irradiance histogram is computed for each data set, then fit to the gamma-gamma distribution using  $\alpha$  and  $\beta$  as the free parameters. The Levenberg-Marquardt<sup>10</sup> algorithm provided by the `lsqcurvefit` function in MATLAB is used for fitting.

The  $C_n^2$  measurements from the Scintec commercial scintillometer are the input to the Andrews model; testing the model requires these to be reliable. As a consistency check, in Figure 3 we compare the predicted irradiance variance from equation (3) to that measured from the link. The measured values are plotted vs. scintillometer  $C_n^2$  readings at the time of the corresponding link measurements. The measured variances are all slightly higher

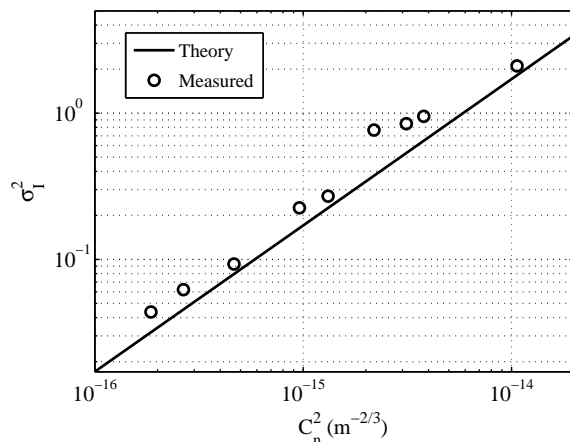


Figure 3: Measured signal variance vs. estimated variance from model using scintillometer provided  $C_n^2$  values.

than those predicted from equation (3). This is true even in saturation, where Rytov theory breaks down and the predicted variance should be an upper bound. Equation (3) is derived for a Kolmogorov spectrum; if the atmosphere matches the Hill spectrum, the bump in power near  $\kappa_l = 2\pi/l_0$  will increase the measured variance. Additional noise sources or tilts error in the system may also contribute, but we believe this effect is minimal.

For the 9 datasets,  $\alpha$  and  $\beta$  vs. measured  $C_n^2$  values are plotted as circles in Figure 4. The lines show the values predicted by the Andrews model using the Kolmogorov spectrum and Hill spectrum with varying values of inner scale.

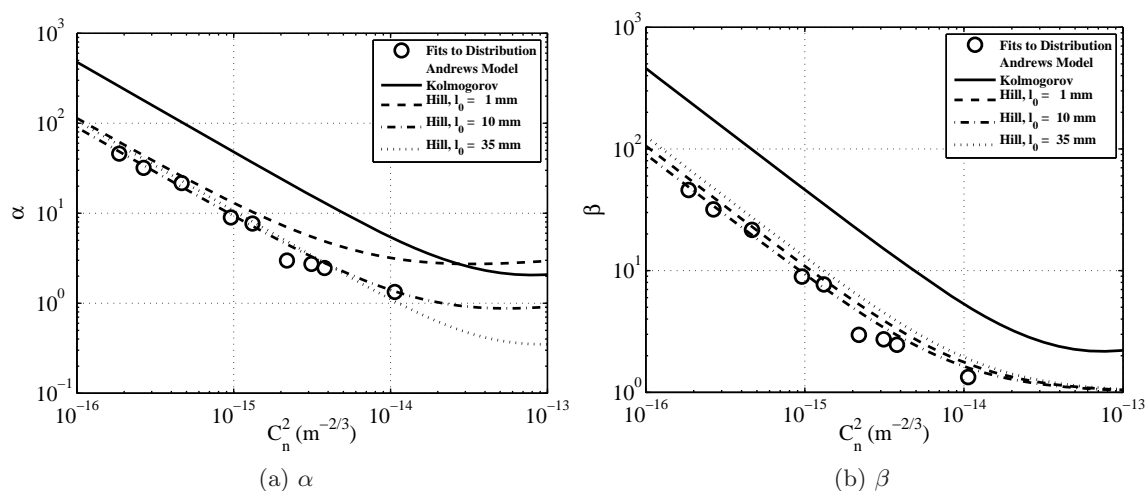


Figure 4:  $\alpha$  and  $\beta$  for gamma-gamma distribution. Fits to data are plotted as circles. Line shows Andrews model predictions using measured  $C_n^2$ .

The fit  $\alpha$  and  $\beta$  values are approximated well using the Andrews model with inner scale  $l_0 = 10 \text{ mm}$ . Our link did not include a measure of inner scale. The literature on near-ground inner scale values is sparse; however,  $10 \text{ mm}$  is on the high end of what one would expect based upon previous measurements.<sup>11,12</sup>

Cumulative distributions of received signal power, along with the gamma-gamma distribution predicted by the Andrews model and gamma-gamma distribution with  $\alpha$  and  $\beta$  values tuned to give the best fit are shown in Figure 5. Plots are shown for 4 of the 9 datasets that span the range of observed turbulence strength. The y-axis is scaled such that a log-normal distribution of received irradiance will appear as a straight line. This allows

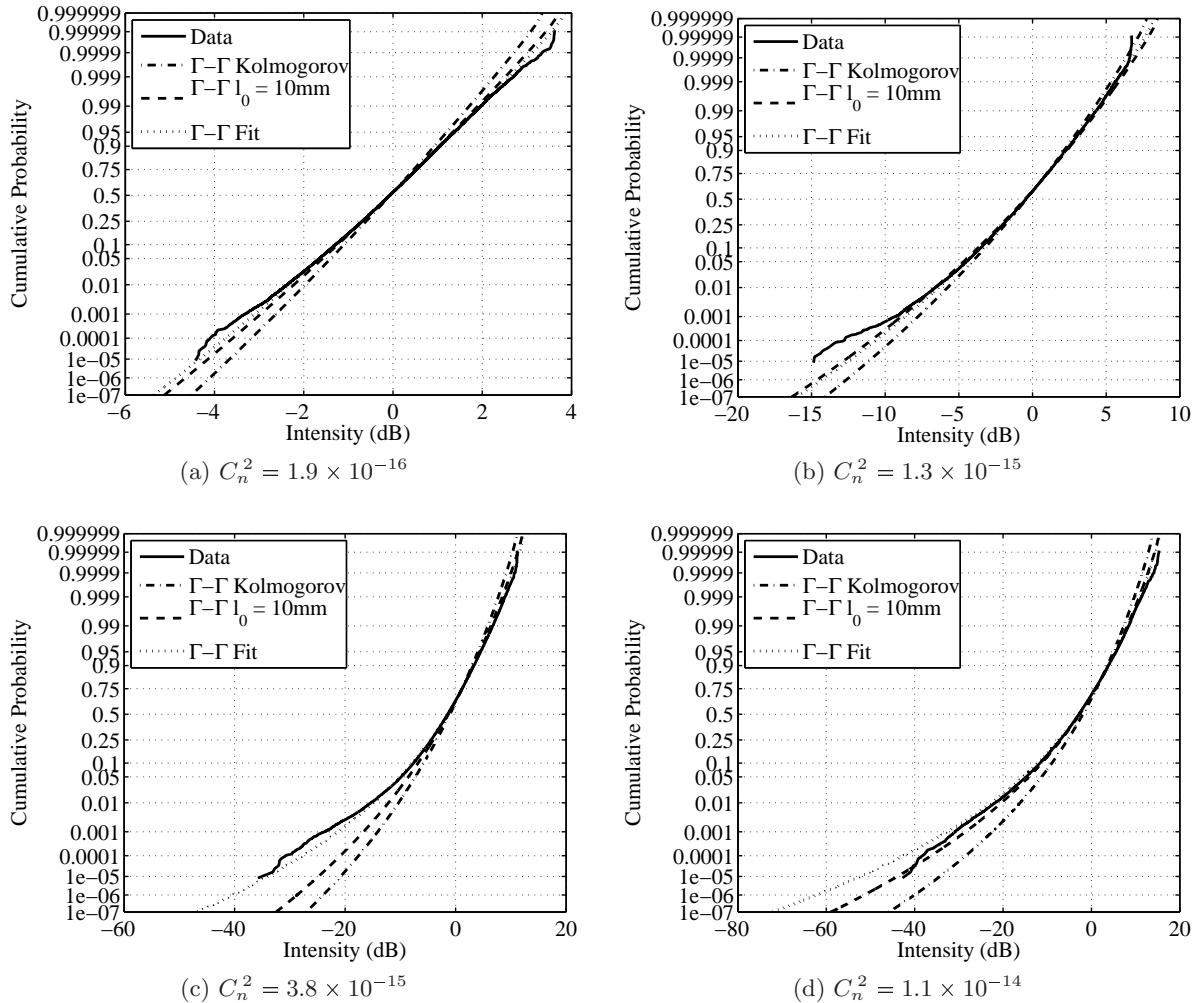


Figure 5: Cumulative probability densities with analytic  $\Gamma$ - $\Gamma$  prediction and  $\Gamma$ - $\Gamma$  fit for Kolmogorov and Hill spectrum with  $l_0 = 10\text{mm}$ . Note that x-axis scales are different for each plot.

for greater resolution at both the high and low extremes of the distribution. The distributions predicted by the Kolmogorov-based model consistently underestimates the probability of deep fades. As noted previously, network outage rates are determined by these low probability events. The model using the Hill spectrum with  $l_0 = 10\text{mm}$  is a better match. Figure 5c shows the largest model deviation; this is the dataset with the 2nd highest  $C_n^2$  measurement. Figure 3 suggests the issue may be a low  $C_n^2$  reading from the scintillometer. The gamma-gamma model with fit  $\alpha$  and  $\beta$  values describe the irradiance distributions well over a wide range of turbulence conditions. Note that the distributions appear log-normal (straight line) for more benign turbulence, but the tails deviate significantly from log-normal and conform well to a gamma-gamma distribution as turbulence strength increases.

## 6. CONCLUDING REMARKS

MIT Lincoln Laboratory has deployed a 5.4km ground-ground optical link that samples at high rate (kHz) the time-varying irradiance produced by atmospheric scintillation. In addition, a commercial scintillometer was used to measure the index of refraction structure function  $C_n^2$ . In this paper, measured data from this link are compared to existing theories for test cases covering two orders of magnitude in  $C_n^2$ . Measured received optical intensity variance agrees with scintillometer-measured  $C_n^2$  assuming constant  $C_n^2$  across the link, as related using equation (3). The cumulative fade distributions over the range of  $C_n^2$  tested are well fit by gamma-gamma distributions. The  $\alpha$ ,  $\beta$  parameters of the gamma-gamma fits are lower than those predicted by Andrews theory



using a Kolmogorov spectrum, but are in reasonable agreement with that theory using a Hill spectrum, for physically relevant values of  $l_0 \cong 10 \text{ mm}$ .

The measured data highlight the deep fades associated with atmospheric scintillation and the potential gain to be obtained in optical communications links by fade mitigation schemes. Absent interleaving, fades at the  $1 \times 10^{-6}$  probability level are 60 dB below the mean for a  $C_n^2$  of  $1 \times 10^{-14} \text{ m}^{-2/3}$ . A combination of interleaving and forward error correction (FEC) that enables robust operation at a CDF of  $3 \times 10^{-3}$  would provide about 30 dB of power margin. Similar power gains can be obtained by aperture averaging or spatial diversity techniques in the optical domain. A clear understanding of the expected fade distribution, particularly in the deep fade tails, is critical for the design of free-space optical communications through strongly turbulent atmospheric channels.

## 7. ACKNOWLEDGMENTS

The authors would like to thank the MIT Westford site staff who supported us, especially Jeff Dominick for hosting our experiment and Jim Hunt for his fearless tower work, the many other staff members of the Advanced Lasercom Systems and Operations group who made this experiment possible, and the Rapid Reaction Technology Office. This work was sponsored by the Department of the Defense under Contract FA8721-05-C-0002. Opinions, interpretations, conclusions, and recommendations are those of the authors and are not necessarily endorsed by the United States Government.

## REFERENCES

- [1] Andrews, L. C., Phillips, R. L., Hopen, C. Y., and Al-Habash, M. A., "Theory of optical scintillation," *J. Opt. Soc. Am. A* **16**(6), 1417–1429 (1999).
- [2] Andrews, L. C., Phillips, R. L., and Hopen, C. Y., [*Laser Beam Scintillation with Applications*], SPIE Press, Bellingham, Washington (2001).
- [3] Al-habash, A., Fischer, K. W., Cornish, C. S., Desmet, K. N., and Nash, J., "Comparison between experimental and theoretical probability of fade for free space optical communications," *Optical Wireless Communications V* **4873**(1), 79–89, SPIE (2002).
- [4] Vetelino, F. S., Young, C., and Andrews, L., "Fade statistics and aperture averaging for gaussian beam waves in moderate-to-strong turbulence," *Appl. Opt.* **46**(18), 3780–3789 (2007).
- [5] Uysal, M., Li, J., and Yu, M., "Error rate performance analysis of coded free-space optical links over gamma-gamma atmospheric turbulence channels," *Wireless Communications, IEEE Transactions on* **5**, 1229–1233 (June 2006).
- [6] Tsiftsis, T., "Performance of heterodyne wireless optical communication systems over gamma-gamma atmospheric turbulence channels," *Electronics Letters* **44**(5), 373–375 (2008).
- [7] Anguita, J., Djordjevic, I., Neifeld, M., and Vasic, B., "Shannon capacities and error-correction codes for optical atmospheric turbulent channels," *J. Opt. Netw.* **4**(9), 586–601 (2005).
- [8] "Boundary layer scintillometers." <http://www.scintec.com/scintibls.htm> (Viewed Dec. 21, 2008).
- [9] Hill, R. J. and Clifford, S. F., "Modified spectrum of atmospheric temperature fluctuations and its application to optical propagation," *J. Opt. Soc. Am.* **68**(7), 892–899 (1978).
- [10] Watson, G. A., ed., [*The Levenberg-Marquardt Algorithm: Implementation and Theory*], *Lecture Notes in Mathematics* **630**, Springer Verlag (1977).
- [11] Hill, R. J. and Ochs, G. R., "Inner-scale dependence of scintillation variances measured in weak scintillation," *J. Opt. Soc. Am. A* **9**(8), 1406–1411 (1992).
- [12] Consortini, A., Cochetti, F., Churnside, J. H., and Hill, R. J., "Inner-scale effect on irradiance variance measured for weak-to-strong atmospheric scintillation," *J. Opt. Soc. Am. A* **10**(11), 2354–2362 (1993).